# B. TECH. PROJECT REPORT

## On

# Fault Diagnosis of Reciprocating Compressors using Artificial Neural Networks


BY

**Nidish Ramakrishnan (130003024)**




**DISCIPLINE OF MECHANICAL ENGINEERING**

**INDIAN INSTITUTE OF TECHNOLOGY INDORE**


**November 2016**

# Fault Diagnosis of Reciprocating Compressors using Artificial Neural Networks

**A PROJECT REPORT**

*Submitted in partial fulfillment of the requirements for the award of the degree*

***of***
**BACHELOR OF TECHNOLOGY**
**in**

**MECHANICAL ENGINEERING**

*Submitted by:*
**Nidish Ramakrishnan (130003024)**

*Guided by:*
**Dr. Anand Parey**


**INDIAN INSTITUTE OF TECHNOLOGY INDORE**
**November 2016**

## CANDIDATE'S DECLARATION

I hereby declare that the project entitled **"Fault Diagnosis of Reciprocating Compressors Using Artificial Neural Networks"** submitted in partial fulfillment for the award of the degree of Bachelor of Technology in 'Mechanical Engineering' completed under the supervision of **Dr. Anand Parey, Associate Professor** ,IIT Indore is an authentic work.

Further, I declare that I have not submitted this work for the award of any other degree elsewhere.

**Nidish Ramakrishnan** **Date-**

---

## CERTIFICATE by BTP Guide(s)

It is certified that the above statement made by the student is correct to the best of my knowledge.

**Signature**

**Dr. Anand Parey**

**Associate Professor,**

**Mechanical Engineering,**

**IIT Indore**

# Preface

*This report on "Fault Diagnosis of Reciprocating Compressors Using Artificial Neural Networks" is prepared under the guidance of Dr. Anand Parey*

*An experimental investigation has been carried out to find the vibration signal characteristics of a reciprocating compressor when it ran under varying frequencies and blockages. I have conducted experiments to find the dependence of two major features, amplitudes of the Fourier transform and energy of the waveform. Using a neural network, accuracies for the different combinations of frequency and amplitudes have been tabulated for future use which is in good accordance with multiple test data.*

*The results obtained from the present experimental study are presented in the tabular form.*

**Nidish Ramakrishnan (130003024)**
B.Tech. IV Year
Discipline of Mechanical Engineering
IIT Indore

# Acknowledgements

First and foremost, I would like to thank my guide Dr. Anand Parey for guiding me thoughtfully and efficiently throughout this project, giving me an opportunity to work at my own pace while providing me with useful directions whenever necessary. I would like to thank Sandeep Patil (PhD scholar) for his constant support and contribution throughout the project. I would also like to thank Vikas Sharma(PhD scholar) for his invaluable support and guidance. I would also like to express gratitude towards the entire solid mechanics lab staff for helping me whole heartedly along the way.

I would also like to take this opportunity to thank my fellow batch mates for being great sources of motivation and for providing encouragement throughout the length of this project.

Finally, I offer my sincere thanks to all other persons who knowingly or unknowingly helped me in completing this project.

**Nidish Ramakrishnan (130003024)**

B.Tech. IV Year

Discipline of Mechanical Engineering

IIT Indore

# Abstract

Condition Monitoring and Fault Diagnosis are very active and important fields of research as they facilitate the reduction of maintenance and reparation costs. Traditional condition monitoring is based on analyzing a specific feature of a vibration signal and understanding the variations observed. Artificial Neural Networks are relatively crude electronic models that can be used for non linear pattern recognition.

An experimental investigation has been carried out in constant frequency condition to study the effect of varying blockage on the characteristics of vibration data of a reciprocating compressor, ½ HP with blocked suction filter provided along with the Machinery Fault Simulator. One tri-axial accelerometer is placed near the discharge valve of the compressor which is connected to a laptop via an analyzer. The frequencies are varied from 10 to 40 Hz in increments of 5 Hz and for each frequency, the blockages are varied from 0 to 80 % in increments of 10 %. The Fourier transforms of the waveforms obtained by the accelerometer are further studied using MATLAB. Using the FFT, the trend of the Fourier transforms is studied and a suitable feature is extracted to be used in classification. From observation, it was found that only a certain band of frequencies is effected when the blockage is increased at a constant compressor RPM. All the blockages are classified using binary algorithm with the base 0% using Artificial Neural Network. It has been observed, blockage with higher degree is classified with higher accuracy when taken with base 0%.

.

# Table of Contents

# List of Figures

# List of Tables

# Chapter 1

# INTRODUCTION

## 1.1General Background

Condition monitoring is the process of monitoring a parameter of condition in a machine element, in order to recognize a significant change which indicates a developing fault. When a certain input parameter goes out of a range of values, the system can be said to be developing a fault. Condition monitoring has a unique benefit in that conditions that would reduce normal lifespan can be addressed before they develop into a major breakdown. These techniques are normally used on rotating elements, with periodic inspection using non-destructive testing techniques.

Temperature gradients across a surface can be discovered with visual inspection and non-destructive testing with thermography. Heat is a sign of developing faults, especially degrading electrical contacts and terminations. Thermography can also be successfully applied to high-speed bearings, fluid couplings, conveyor rollers, and storage tank internal build-up.

Ultrasound can be used for high-speed and slow-speed mechanical applications and for high-pressure fluid situations. Digital ultrasonic meters measure high frequency signals from bearings and display the result as a dBuV (decibels per microvolt) value. This value is trended over time and used to predict increases in friction, rubbing, impacting, and other bearing defects. The dBuV value is also used to predict proper intervals for re-lubrication. Ultrasound monitoring, if done properly, proves out to be a great companion technology for vibration analysis.

Most vibration analysis instruments today utilize a Fast Fourier Transform (FFT) which is a special case of the generalized Discrete Fourier Transform and converts the vibration signal from its time domain representation to its equivalent frequency domain representation.

This report will mainly deal with vibration signals.

## 1.2 Compressor

A gas compressor is a mechanical device that increases the pressure of a gas by reducing its volume. An air compressor is a specific type of gas compressor. Compressors are similar to pumps: both increase the pressure on a fluid and both can transport the fluid through a pipe. It converts power (using an electric motor,

diesel or gasoline engine, etc.) into potential energy stored in pressurized air (i.e., compressed air). By one of several methods, an air compressor forces more and more air into a storage tank, increasing the pressure.

## 1.3 Types of compressors

### 1.3.1 Reciprocating

Reciprocating air compressors are positive displacement machines, meaning that they increase the pressure of the air by reducing its volume. This means they are taking in successive volumes of air which is confined within a closed space and elevating this air to a higher pressure. The reciprocating air compressor accomplishes this by a piston within a cylinder as the compressing and displacing element.

### 1.3.2. Rotatary Screw

Rotary air compressors are positive displacement compressors. The most common rotary air compressor is the single stage helical or spiral lobe oil flooded screw air compressor. These compressors consist of two rotors within a casing where the rotors compress the air internally. There are no valves. These units are basically oil cooled (with air cooled or water cooled oil coolers) where the oil seals the internal clearances.

### 1.3.3. Centrifugal

The centrifugal air compressor is a dynamic compressor which depends on transfer of energy from a rotating impeller to the air. Centrifugal compressors produce high-pressure discharge by converting angular momentum imparted by the rotating impeller (dynamic displacement). In order to do this efficiently, centrifugal compressors rotate at higher speeds than the other types of compressors. These types of compressors are also designed for higher capacity because flow through the compressor is continuous.

## 1.4 Types of faults in compressors

1. Leaking Valve- This occurs when there is gas leaking out of the compressor valve, either the discharge of the inlet.

Cause- Main cause of this type of fault is mechanical looseness in the discharge fastenings or breakage in the valves.

Solution- Looseness can be solved by tightening the bolts and replacement is the solution when it comes to breakage.

2. Blockages in discharge- This occurs when there is blockage in the discharge section of the compressor which prevents or restricts air flow and causes mechanical vibrations and noise.

Cause- The major cause of this type of fault is bad quality of air used which causes particles to deposit in the discharge of compressor and thus producing a blockage to air flow. Another cause of blockage can be breakage of a component in the discharge section getting sucked up to the discharge orifice and choking it up.

Solution- This can be solved by cleaning the effected section of the compressor using a compressed air blow or a solvent solution or removing the broken part from the discharge orifice.

## 1.5 Artificial Neural Networks

An artificial neural network is an interconnected group of nodes, similar to the vast network of neurons in a brain. Here, each node signifies an artificial neuron and an arrow represents a connection from the output of one neuron to the input of another. Each node in the next layer is connected to each node in its previous layer by a weight. Value of each node can be found by summation of product of the value of the node by the corresponding weight. The lesser the weight, more is the generalization property of the network. The weights are determined by using the training data sets that are available, and in validating, the errors are minimized and network is further optimized in algorithms such as back propagation.

Back propagation, an abbreviation for "backward propagation of errors", is a very popular method of training that is used along with an optimization method such as gradient descent. It calculates the change of a loss function (function that maps the errors into a real number) with respect to all the weights in the network; so that the gradient is fed to the optimization method which in turn uses it to update the weights, in an attempt to minimize the loss function. The ANN used is a binary classifier with input, hidden and output layer having 1,2 and 2 neurons respectively.

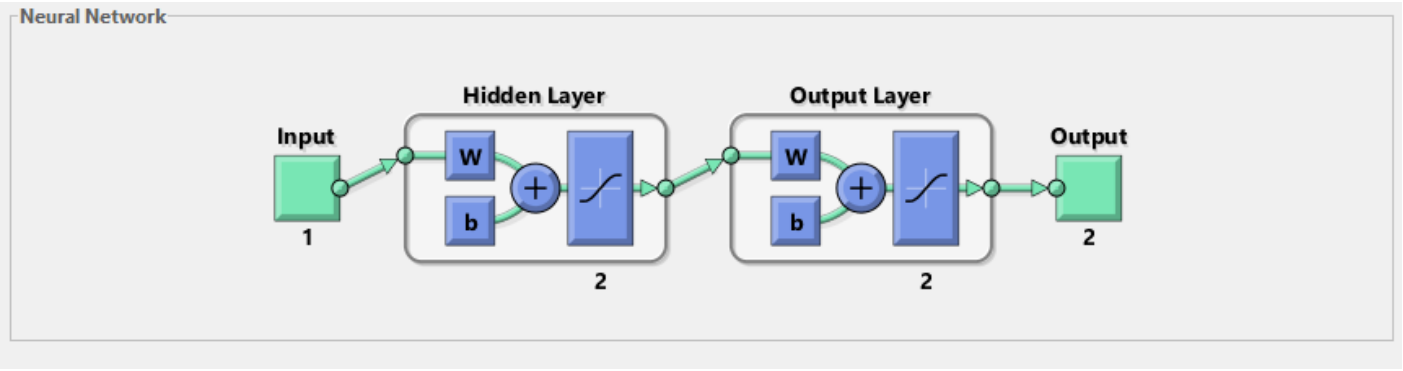


Figure 1.1 Structure of the ANN used

**Calculation of weights and minimization of errors (Delta Rule)**

The calculation of weights and optimization process is done by the Neural Network toolbox in MATLAB. The mathematical way of doing it manually is as follows,

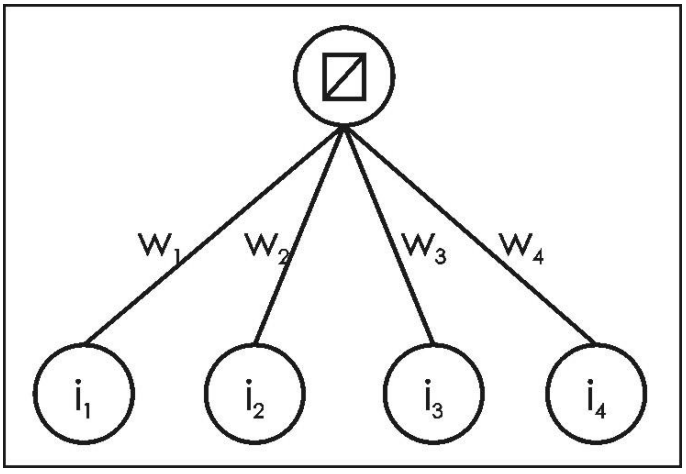


Figure 1.2 Relation between output of successive node with previous layer [38]

(Equation 1a)

$$S_j = \sum_i w_{ij} a_i \tag{1a}$$

and

(Equation 1b)

$$a_j = f(S_i) \tag{1b}$$

where Sj is the sum of all corresponding products of weights and outputs from the previous layer i, $w_{ij}$ represents the relevant weights connecting layer i with layer j, $a_i$ represents the activations of the nodes (output corresponding to the set of inputs) in the previous layer i, $a_j$ is the activation of the node at hand, and f is the activation function.

Delta Rule employs the error function, which involves the adaptation of weights along the most direct path in weight-space to minimize error; change applied to a given weight is proportional to the negative of the derivative of the error with respect to that weight. The error function is commonly given as the sum of the squares of the differences between all target and actual node activations for the output layer. For a particular training pattern (i.e., training case), error is thus given by:

(Equation 2a)

$$E_p = \frac{1}{2}\sum_n (t_{j_n} - a_{j_n})^2 \qquad (2a)$$

where $E_p$ is total error over the training data sets, ½ is a number applied to simplify the function's derivative, n represents all output nodes for a given training data set, $t_j$ sub n represents the target value for node n in output layer j, and $a_j$ sub n represents the actual activation for the same node. This particular error measure is striking because its derivative, whose value is imperative for use of the Delta Rule, is easily calculated. Error over an entire set of training patterns (i.e., over one iteration, or epoch is calculated by summation of all Eps:

(Equation 2b)

$$E = \sum_p E_p = \frac{1}{2}\sum_p \sum_n (t_{j_n} - a_{j_n})^2 \qquad (2b)$$

where E is total error, and p represents all training patterns. An equivalent term for E in Equation 2b is sum-of-squares error. A normalized version of Equation 2b is given by the mean squared error (MSE) equation:

(Equation 2c)

$$MSE = \frac{1}{2PN}\sum_p \sum_n (t_{j_n} - a_{j_n})^2 \qquad (2c)$$

where P and N are the total number of training patterns and output nodes, respectively. It is the error of Equations 2b and 2c that gradient descent attempts to minimize.

## 1.6 Review of literature

Modern industrial facilities are heavily automated and instrumented; consequently there is a lot of process data available which can be used to monitor the condition of the system. The difficulties attached to the development of accurate and reliable first-principle models of large and complex industrial facilities have motivated the development of data driven monitoring algorithms such as Principal Component Analysis (PCA), Partial Least Squares (PLS) or Canonical Variate Analysis (CVA) [1]. Literature gives examples of extensive application of these methods for detection and diagnosis of faults using computer simulated data [2–5] or real data obtained from industrial facilities or experimental test rigs [6–12].

Despite their success, PCA and PLS(and their corresponding dynamic approaches known as Dynamic PCA and Dynamic PLS [13,14]) have been reported not to be as efficient as othe rstate-space based methodologies such as Canonical Variate Analysis(CVA).The benefits of CVA are especially relevant when applied to systems working under variable loading conditions, principally due to their presentation of the system dynamics [2,15,16].

The simplest and most commonly used method for detecting the presence of faults using vibration analysis involves the comparison of different signal features (such as RMS value, peak amplitude) in the measured signal against a machine working under healthy conditions. Assuming that the initial status of the machine was healthy, any changes in the measured feature response may be assumed to be due to the deterioration of the machine condition. However, this assumption is only valid if all the measurements are taken under the same loading conditions, as different levels of load will generate different vibration levels [17].

It is possible to find in literature some examples of techniques used to monitor the condition of machines working under variable loading conditions using vibration data. McFadden [18, 19] proposed a method based on band pass filtered time- domain synchronous averaging (TSA) and the Hilbert transform, with Kurtosis being used as an indicator of fault severity. However there are some disadvantages in this technique due to the requirement of the user to configure the bandwidth for the band-pass filter [20].

Other methods are based on the examination of time-frequency maps where the instantaneous power spectrum is represented [21], but this method does not produce a single indicator of the machine condition that can be tracked in time. Parker Jr. et al. [22] proposed a method based on change detection in the bispectral domain which produced severity indicators which are independent of the loading conditions.

However, the method requires long computational times. The work presented by Zhan et al. [23] proposes a technique based on motion residuals, which are calculated as the difference between the TSA of a signal and the average vibration observed in the healthy state under different loading conditions. This area has gained importance in the last years and Braun [24] reviewed the state of the art of vibration diagnostics using TSA in 2011. Other methodologies presented recently are based on capturing the correlation between features extracted from the vibration signal and the operating conditions. This kind of approach has been applied successfully for diagnostics of planetary gearboxes in a bucket wheel excavator [25] and wind turbine bearing diagnostics [26].

[28–29] present the feature extraction method of vibration signals using time frequency techniques for fault diagnosis of rotating machinery. Model- based FDD methods have been employed for centrifugal chiller system and gas turbine [30, 31]. Fuzzy logic based FDD methods are also developed for diagnosis of gas turbine [32,33] and centrifugal compressor [37]

The application of machine learning methods like artificial neural networks (ANN) and support vector machine (SVM) in rotating machinery fault diagnosis are presented in [38,39].

## 1.7 Scope of Dissertation

1. Fault diagnosis of Blockages in reciprocating compressors has not been conducted in the literature.
2. Use of Artificial Neural Networks not studied much in this aspect.

# Chapter 2

# Fault Diagnosis of Reciprocating Compressors Using Artificial Neural Networks

## 2.1 Introduction

The objective of the present study is to use Artificial Neural Networks to help in the fault diagnosis process of reciprocating compressors. Here, a faulty compressor given in the faulty compressor kit of the MFS (Machinery Fault Simulator) is used. An accelerometer is used that is connected near the discharge section of the compressor which records the vibrations and sends it to a laptop. A total of 63 Tests have been carried out for different value of frequency (0-40 Hz, increments of 5Hz) and blockages (0-80%, increments of 10%). Energy of the waveform is extracted from each sets and fed into an ANN (Artificial Neural Network). The accuracy achieved in classifying the different blockages with the base (0% blockage) for each frequency is noted. The implications of the accuracies achieved are discussed.

## 2.2 Experimental Setup and Procedure

### 2.2.1 Test facility

The main apparatus being used to perform the experiments is the MFS or the machinery fault simulator. It is manufactured by Spectra Quest inc. and comes with attachments and provisions to use different combinations of couplings, components and make them operate at different frequencies. The MFS is shown labelled in figure 2.1 along with the different components that are attached to it.

The schematic view of the test facility developed for the present investigation is shown in Figure 2.1. The test facility consists machinery fault simulator which consists of a compressor, air tank, power supply system, motor and additional accelerometer, connecting wires, analyzer and laptop. A ½ HP reciprocating compressor has been used as the rotator component in this study. The component is fixed as shown in figure 2.2 to the MFS (Spectra Quest Inc.) on a sliding plate that can be used to tighten the belt which drives the compressor. The bottom plate is then tightened using bolts so that it stays affixed to the MFS. The compressor is connected to a belt that couples it with the rod that is connected to the motor of the MFS. A tri-axial accelerometer (as shown in figure 2.2) is connected to the discharge section of the compressor using wax. The accelerometer is connected to an analyser (figure 2.4) using connecting wire. The analyser (figure 2.4) is connected to the laptop using a LAN cable which has the NV gate software for recording the vibration signals. The frequency of the compressor can be controlled using a control box (SMV Tech, Lenze AC) (figure 2.3) that is mounted on the MFS. The maximum permissible frequency under which the compressor

can operate is 55 Hz. The air tank (figure 2.5) of the compressor kit is attached to the compressor using the air tube and before performing the experiment the inlet valve of the air tank is opened so that air can flow from the compressor.

There are 4 bolts on the top section of compressor under which a plate with flap is provided. The flap blocks the path of air coming out of the discharge section as shown in figure. This flap (figure 2.6) simulates the presence of a blockage in the compressor discharge. A screw is present on the flap that controls the degree of blockage by moving the flap closer or away from the discharge orifice. The blockages are classified according to the displacement of the screw. When the flap completely blocks the discharge section, the blockage is said to be 100% and the displacement of the screw in radians is noted. Then the flap is taken to the maximum possible distance away from the orifice and the blockage and displacement are made to be 0 at this point. The blockages are linearly graded with the displacement of the screw.

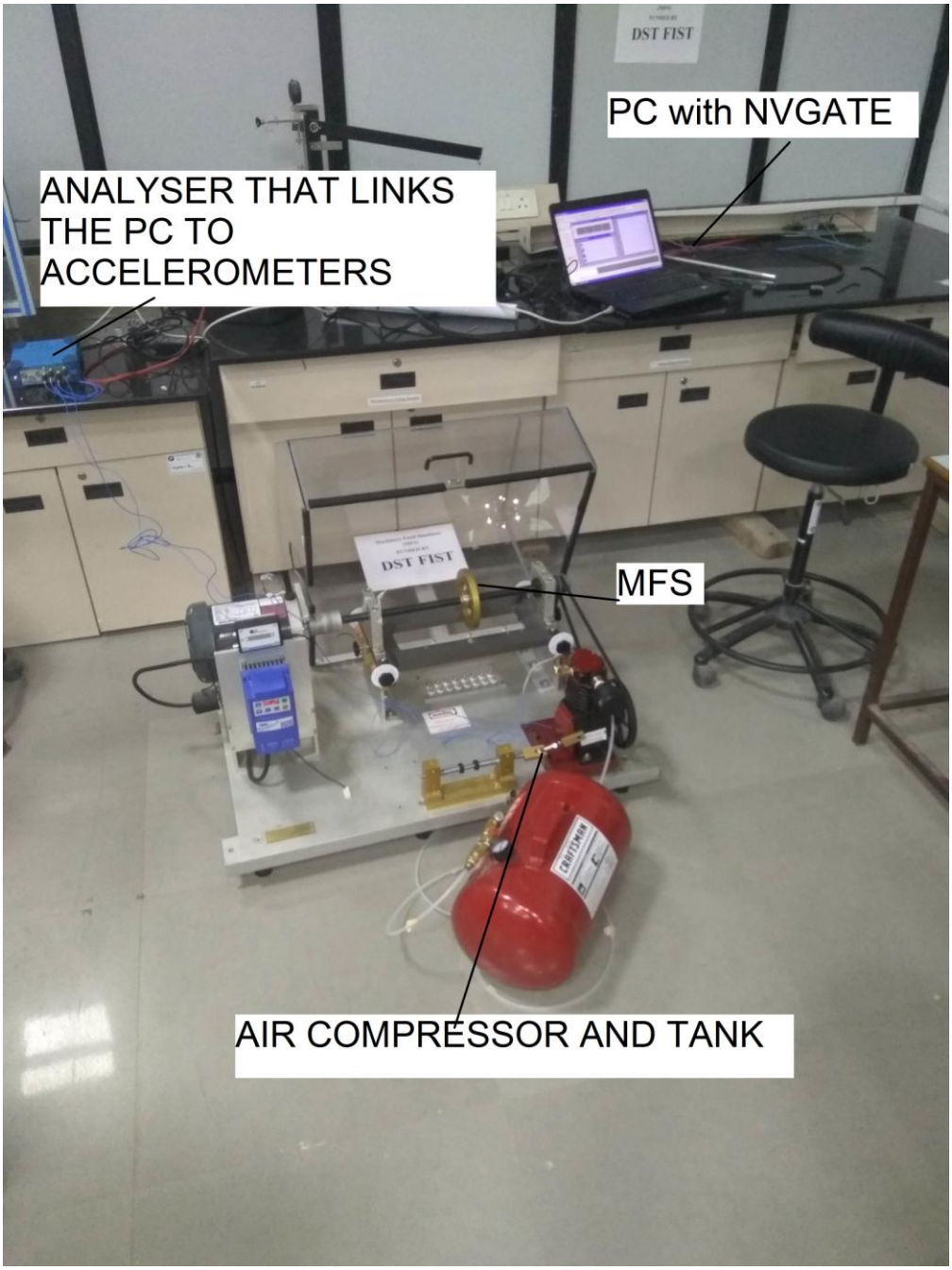


Figure 2.1.Experimental Setup

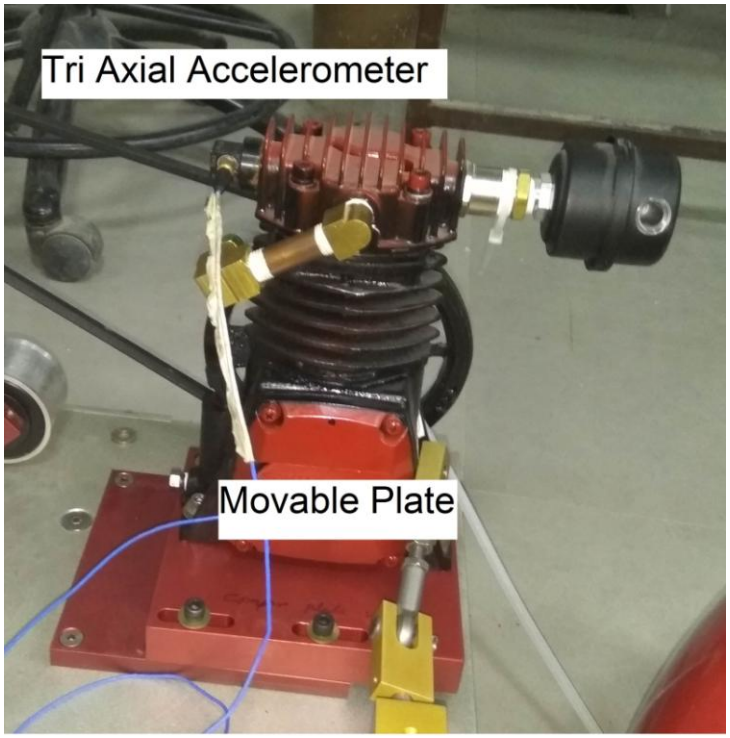


Figure 2.2. -Position of Tri Axial Accelerometer and compressor plate


Figure 2.3. Control Box(SMV Lenze AC Tech)

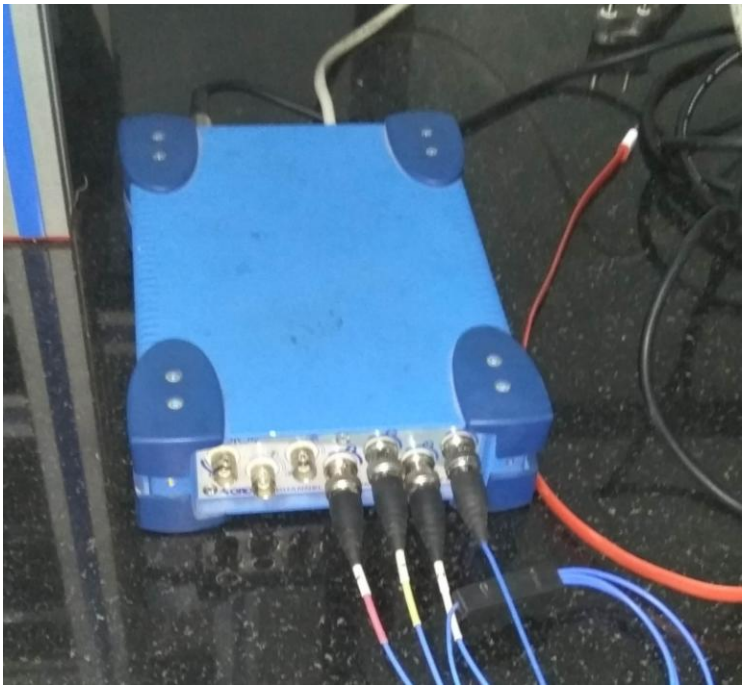

Figure 2.4. Analyzer


Figure 2.5. Air Tank

Figure 2.6. Restricted discharge orifice

2.2.2Experimental procedure and data reduction

Tests are carried out at room temperature and atmospheric pressure in the present investigation. Two parameters: frequency of compressor and degree of blockage are present in the experimental investigation (Table 2.1). The rotational speed of the compressor is controlled by the control box to provide the desired flow rate of air. Air is directed into the air tank in which pressure develops eventually. First, a time of 10 secs is given to the compressor to set into steady state. The compressor is run for 20 secs after achieving steady state and the NV gate software is calibrated to give out 50 data sets in the given time.

The accelerometer (ACC301) used in the present investigation is having a sensitivity of 10.57 $mV/(m/s^2)$.

During experiments, three trial runs are conducted to check the working of the accelerometer. The range of operating parameters considered in the present experimental study is listed in Table 2.3. The run time is considered and the belt is checked for cases of overheating.

The sampling frequency for MATLAB Operations is kept at 1024 Hz.

Table 2.1 Experimental Plan

| | | | | Frequencies | | | | |
|---|---|---|---|---|---|---|---|---|
| | | 10 HZ | 15 HZ | 20 HZ | 25 HZ | 30 HZ | 35 HZ | 40 HZ |
| | 0% | 0%,10HZ | 0%.15HZ | 0%.20HZ | 0%.25HZ | 0%.30HZ | 0%.35HZ | 0%.40HZ |
| | 10% | 10%,10HZ | 10%,15HZ | 10%,20HZ | 10%,25HZ | 10%,30HZ | 10%,35HZ | 10%,40HZ |
| | 20% | 20%,10HZ | 20%,15HZ | 20%,20HZ | 20%,25HZ | 20%,30HZ | 20%,35HZ | 20%,40HZ |
| Blockage | 30% | 30%,10HZ | 30%,15HZ | 30%,20HZ | 30%,25HZ | 30%,30HZ | 30%,35HZ | 30%,40HZ |
| | 40% | 40%,10HZ | 40%,15HZ | 40%,20HZ | 40%,25HZ | 40%,30HZ | 40%,35HZ | 40%,40HZ |
| | 50% | 50%,10HZ | 50%,15HZ | 50%,20HZ | 50%,25HZ | 50%,30HZ | 50%,35HZ | 50%,40HZ |
| | 60% | 60%,10HZ | 60%,15HZ | 60%,20HZ | 60%,25HZ | 60%,30HZ | 60%,35HZ | 60%,40HZ |
| | 70% | 70%,10HZ | 70%,15HZ | 70%,20HZ | 70%,25HZ | 70%,30HZ | 70%,35HZ | 70%,40HZ |
| | 80% | 80%,10HZ | 80%,15HZ | 80%,20HZ | 80%,25HZ | 80%,30HZ | 80%,35HZ | 80%,40HZ |

### 2.2.3 Vibration data and waveform

A sample of the vibration data set obtained during experimental study by using from the NV gate software is detailed below.

Table 2.2 Sample data at 0% blockage, 10Hz

| Time (ms) | Acceleration | Time (ms) | Acceleration | Time (ms) | Acceleration | Time (ms) | Acceleration |
|---|---|---|---|---|---|---|---|
| 0 | 2.44E-01 | 35.82225 | 5.68E-01 | 17.67231 | 5.89E-01 | 53.97219 | -1.17E-01 |
| 0.47763 | 1.00E+00 | 36.29988 | 1.22E-01 | 18.14994 | 3.51E-01 | 54.44982 | -7.46E-01 |
| 0.95526 | 4.31E-01 | 36.77751 | -4.78E-01 | 18.62757 | 5.97E-01 | 54.92745 | -3.50E-01 |
| 1.43289 | 4.64E-01 | 37.25514 | -3.42E-01 | 19.1052 | 1.93E-01 | 55.40508 | 4.20E-01 |
| 1.91052 | 7.75E-01 | 37.73277 | -6.75E-01 | 19.58283 | 6.58E-01 | 55.88271 | 3.27E-01 |
| 2.38815 | 5.48E-01 | 38.2104 | -7.49E-01 | 20.06046 | 7.27E-02 | 56.36034 | -6.10E-01 |
| 2.86578 | -2.75E-01 | 38.68803 | -1.16E+00 | 20.53809 | -1.68E+00 | 56.83797 | -3.99E-02 |
| 3.34341 | 1.46E-01 | 39.16566 | -9.76E-01 | 21.01572 | 9.98E-02 | 57.3156 | -4.15E-02 |
| 3.82104 | -1.08E-01 | 39.64329 | -7.99E-03 | 21.49335 | -2.69E-01 | 57.79323 | 2.84E-02 |
| 4.29867 | -9.31E-01 | 40.12092 | -1.23E+00 | 21.97098 | -2.99E-01 | 58.27086 | -2.26E-01 |
| 4.7763 | -3.92E-01 | 40.59855 | -9.39E-01 | 22.44861 | -2.93E-01 | 58.74849 | 2.44E-01 |
| 5.25393 | -3.55E-02 | 41.07618 | -6.22E-01 | 22.92624 | 8.87E-01 | 59.22612 | -5.03E-01 |
| 5.73156 | 6.92E-01 | 41.55381 | -3.10E-01 | 23.40387 | 6.42E-01 | 59.70375 | 8.76E-01 |
| 6.20919 | -7.66E-01 | 42.03144 | -7.53E-02 | 23.8815 | -1.10E+00 | 60.18138 | 9.19E-01 |
| 6.68682 | -3.21E-01 | 42.50907 | 5.03E-02 | 24.35913 | -5.75E-01 | 60.65901 | 3.46E-01 |
| 7.16445 | -9.59E-01 | 42.9867 | 4.83E-01 | 24.83676 | 8.67E-02 | 61.13664 | 8.33E-01 |
| 7.64208 | -2.08E-01 | 43.46433 | 9.00E-01 | 25.31439 | -1.26E-01 | 61.61427 | 6.13E-01 |
| 8.11971 | 2.67E-01 | 43.94196 | 1.06E+00 | 25.79202 | 4.74E-01 | 62.0919 | 6.70E-01 |
| 8.59734 | 4.63E-01 | 44.41959 | 7.08E-01 | 26.26965 | 6.23E-02 | 62.56953 | 3.89E-01 |
| 9.07497 | 2.67E-01 | 44.89722 | -1.21E-01 | 26.74728 | 5.10E-01 | 63.04716 | 7.52E-01 |
| 9.5526 | 1.31E-01 | 45.37485 | 1.09E+00 | 27.22491 | -3.67E-01 | 63.52479 | 8.60E-01 |
| 10.03023 | 3.02E-01 | 45.85248 | 1.41E+00 | 27.70254 | -6.69E-01 | 64.00242 | 1.81E-01 |
| 10.50786 | -1.52E+00 | 46.33011 | 8.71E-01 | 28.18017 | -2.84E-01 | 64.48005 | 5.31E-02 |
| 10.98549 | -1.16E+00 | 46.80774 | 5.03E-01 | 28.6578 | -4.86E-01 | 64.95768 | 5.34E-02 |
| 11.46312 | 4.08E-01 | 47.28537 | 4.44E-01 | 29.13543 | 2.75E-01 | 65.43531 | 1.83E-01 |
| 11.94075 | 3.35E-01 | 47.763 | 4.93E-01 | 29.61306 | 7.51E-01 | 65.91294 | -1.44E-01 |
| 12.41838 | -6.28E-01 | 48.24063 | 2.20E-01 | 30.09069 | 3.42E-01 | 66.39057 | 5.76E-02 |
| 12.89601 | 9.95E-02 | 48.71826 | 4.15E-01 | 30.56832 | -1.57E-01 | 66.8682 | -2.20E-01 |
| 13.37364 | 1.80E-01 | 49.19589 | -2.85E-01 | 31.04595 | 1.38E-01 | 67.34583 | -3.07E-01 |
| 13.85127 | -5.71E-01 | 49.67352 | 1.22E+00 | 31.52358 | 6.87E-01 | 67.82346 | 8.92E-02 |
| 14.3289 | -6.88E-02 | 50.15115 | -6.17E-01 | 32.00121 | 1.19E-01 | 68.30109 | -4.47E-01 |
| 14.80653 | 1.03E+00 | 50.62878 | 2.02E-01 | 32.47884 | 5.64E-01 | 68.77872 | -5.24E-01 |
| 15.28416 | 1.35E+00 | 51.10641 | -8.12E-01 | 32.95647 | 7.52E-01 | 69.25635 | -6.64E-01 |
| 15.76179 | 5.22E-01 | 51.58404 | -6.80E-02 | 33.4341 | 9.72E-01 | 69.73398 | -2.68E-01 |
| 16.23942 | 8.18E-01 | 52.06167 | 4.25E-01 | 33.91173 | 8.96E-01 | 70.21161 | -1.44E-01 |
| 16.71705 | 1.05E+00 | 52.5393 | -1.25E+00 | 34.38936 | 1.52E-01 | 70.68924 | 1.21E-01 |
| 17.19468 | -1.01E+00 | 53.01693 | -9.29E-01 | 34.86699 | 6.38E-01 | 71.16687 | -2.20E-01 |

This raw vibration data in time domain was converted into frequency domain in MATLAB. Samples of graph of raw data and Fourier transform given below,

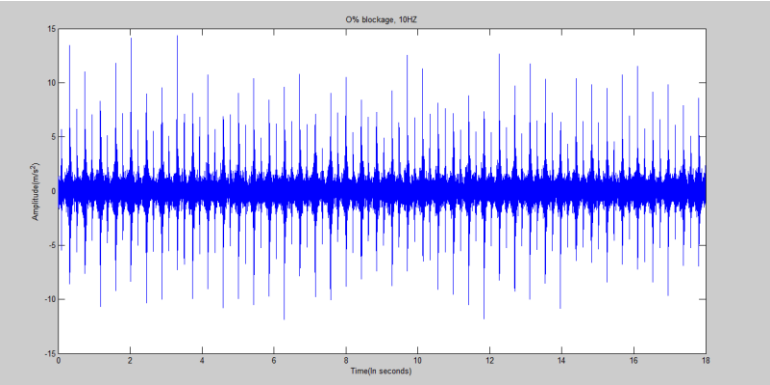


Figure 2.7 Raw signal for 0% blockage, 10 Hz

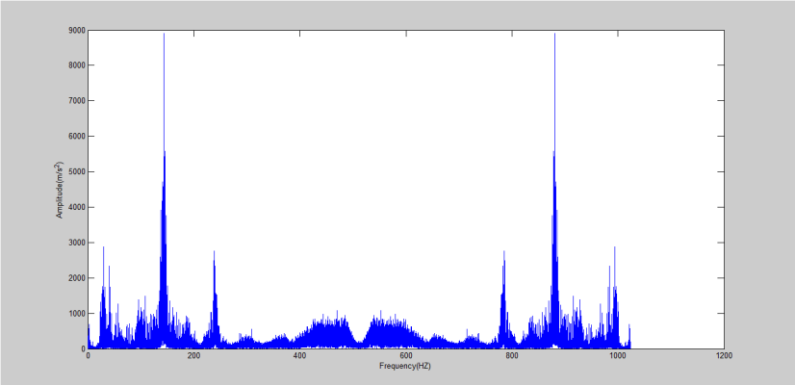


Figure 2.8 Frequency domain signal for 0% blockage, 10 Hz

2.2.4 Feature extraction

After looking at the trends in the graphs in frequency domain, it was seen that the amplitudes of a certain frequency range(400-600 Hz) increase with increase in blockage, for a constant frequency. Taking this fact into consideration, energy feature (sum of squares of amplitudes multiplied by the signal duration) of the wave is extracted.

$$E = T \sum_{n-0}^{N-1} x^2[n]$$

This energy is used as the input parameter in the ANN. While classifying, 0% blockage is given an output of 0 and the blockage to be classified is given an output of 1 and classification is carried out.

### 2.2.5 Neural Network Toolbox interface

The classification is done in the neural network toolbox. The toolbox interface for a test case is shown below,

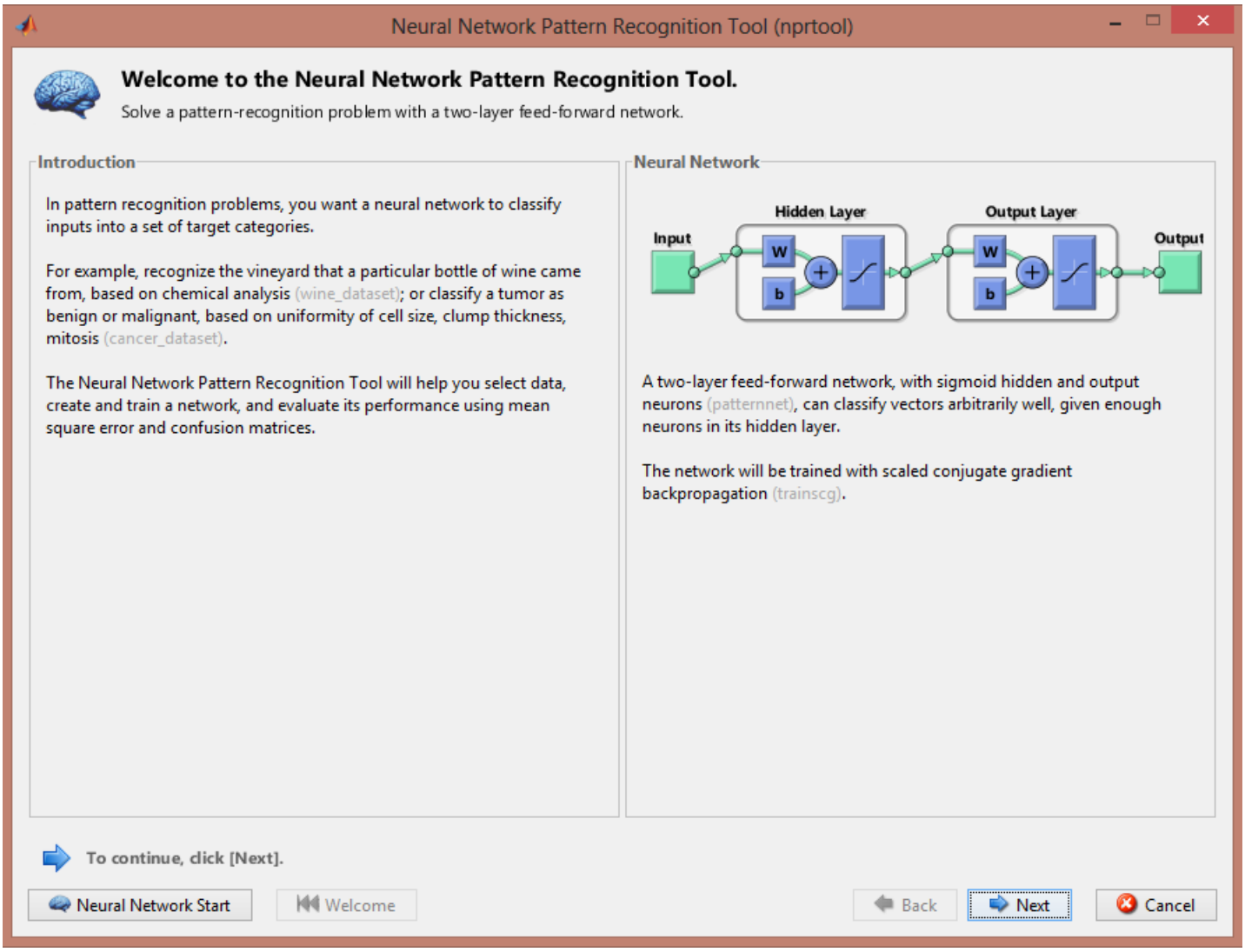


Figure 2.9 Startup page for test case (0%, 10 Hz)

The start page for the neural network pattern recognition tool,

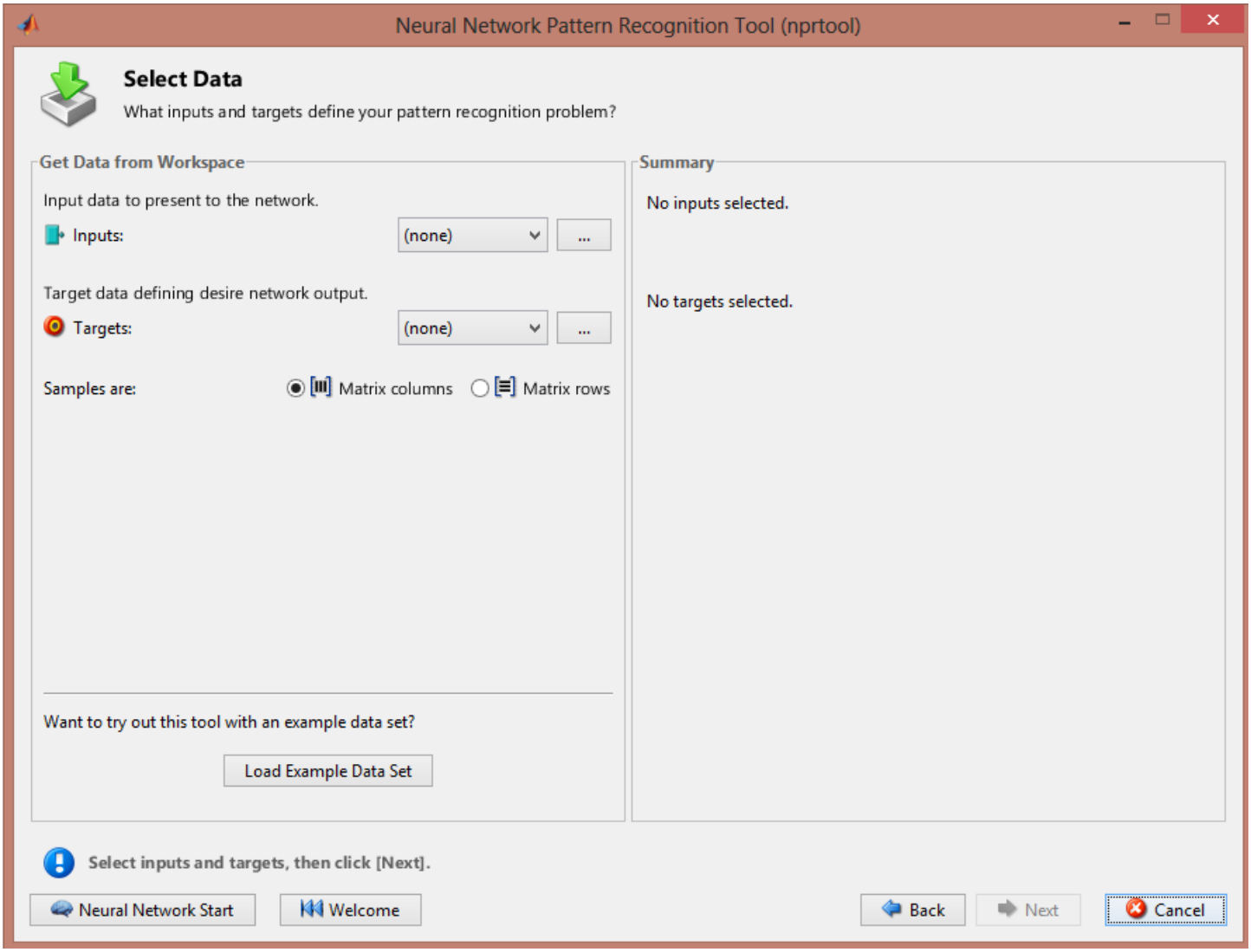


Figure 2.10 Input/output page for test case(0%, 10Hz)

Here you select the input and output matrices from the drop down menu. The output is usually a matrix containing an array of 0's and 1's aligned with the corresponding inputs.

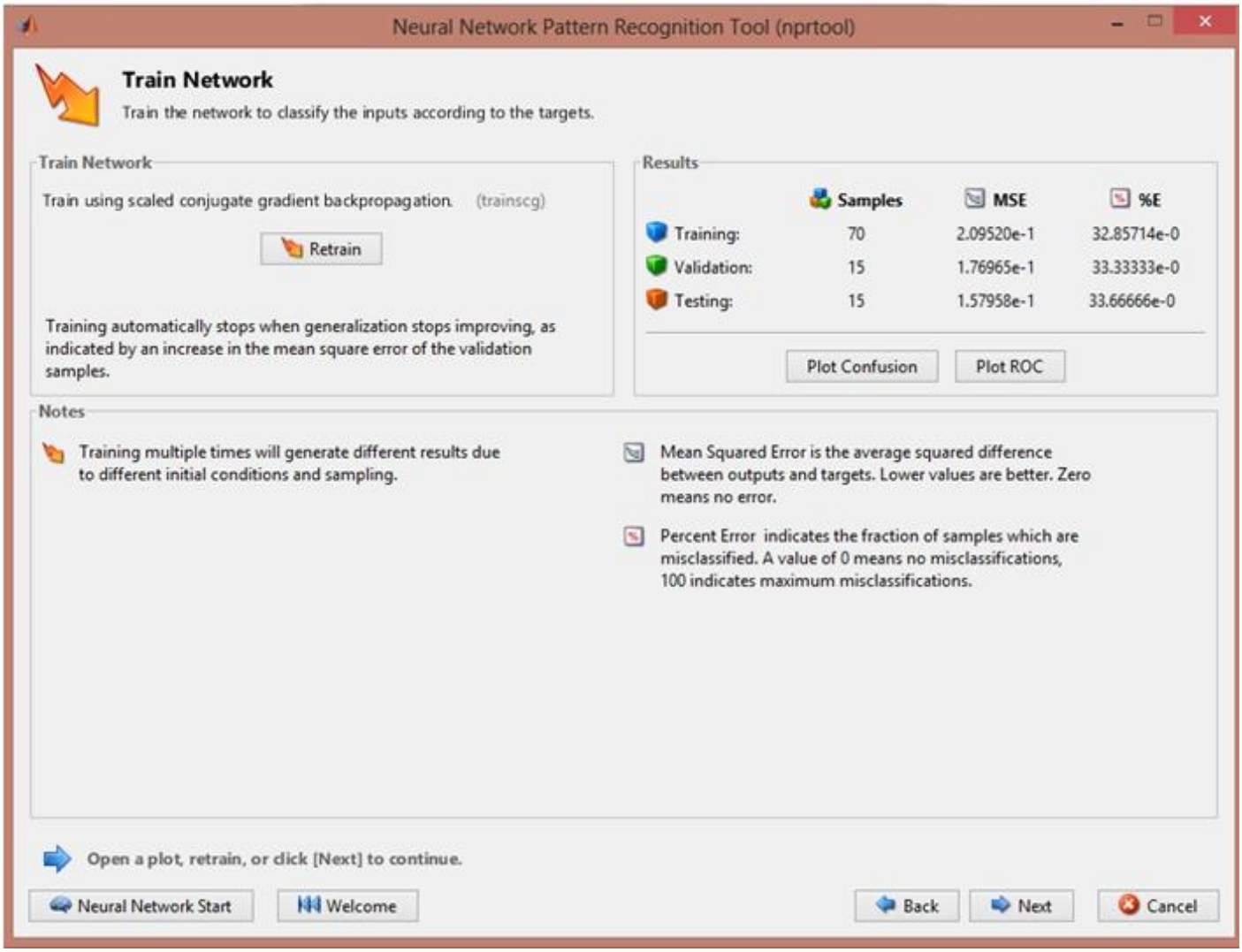


Figure 2.11 Training/Results page for test case(0%, 10 Hz)

This is the view after one round of training is done. When you click on train, the network trains itself using the data that you input. This being a back propagation algorithm validates and tries to retrain using the errors found in validation. The training, validation and testing errors and mean squared errors are shown on the right hand side. The errors found here for each test case is noted and the accuracies are calculated by subtracting from 100.

In the beginning, multi-class ANN was considered for use in the classification but looking at the number of classes (5 classes) and the fact that all the signals were not that different from each other(the 0% and 10% signal were similar and so were the 10% and 30% signals), that idea was scrapped. Instead all the blockages were taken with base 0% and classified using binary ANN. Now what this did was, this used the similarity of the waves with base 0% instead of using the difference. A lower percentage blockage like 10% and 30% will

be more similar to the 0% blockage signal than say 50% or 70% and hence they can be classified on the basis of their classification accuracies. So the accuracies of each pair were tabulated and an increasing trend in accuracies on increasing the blockage was observed as discussed.

So the classification can be said to be of the form ‘nnclass (b0, bx)’,

Where nnclass is the neural network classifier function, b0 and bx are the matrices containing the energy values of blockage 0% and x% (x=10, 30, 50, 70) at a particular frequency.

The results and observations are listed in the next section.

# Chapter 3

# RESULTS AND DISCUSSIONS

## 3.1 Vibration data and Fourier transform characteristics

Looking at the graphs, it can be seen that a particular band of frequencies increases with increase in the blockage. The graphs for the Fourier transform of the vibration data for a constant frequency are given below.

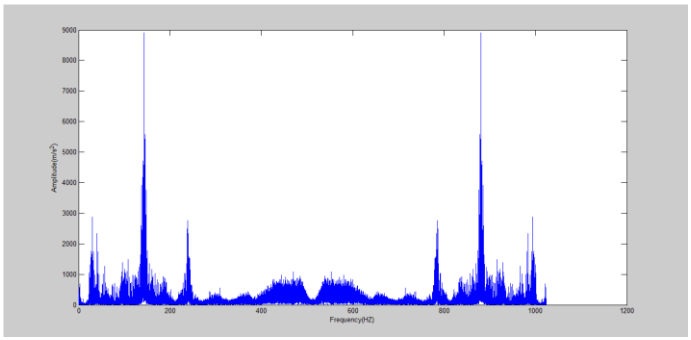


Figure 3.1 FFT plot (0% blockage, 10 Hz)

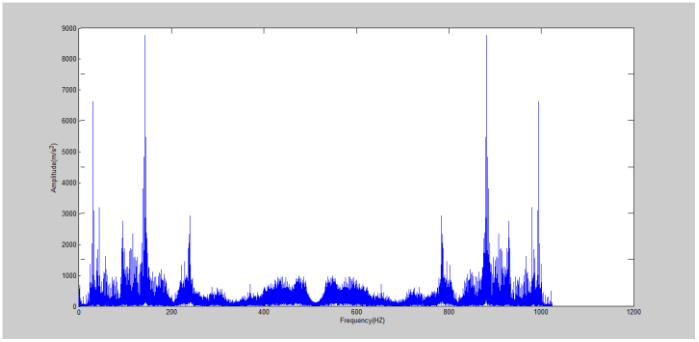


Figure 3.2 FFT plot(10% blockage, 10 Hz)

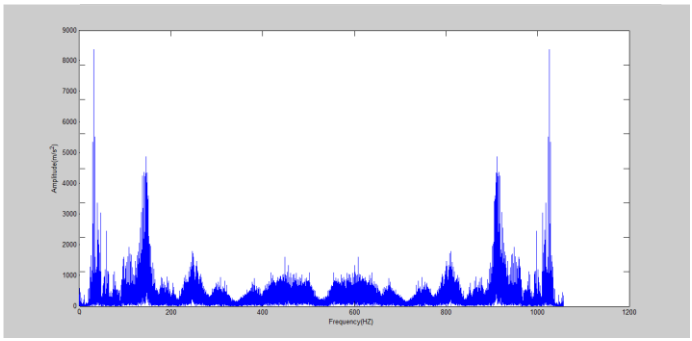


Figure 3.3 FFT plot (20% blockage, 10 Hz)

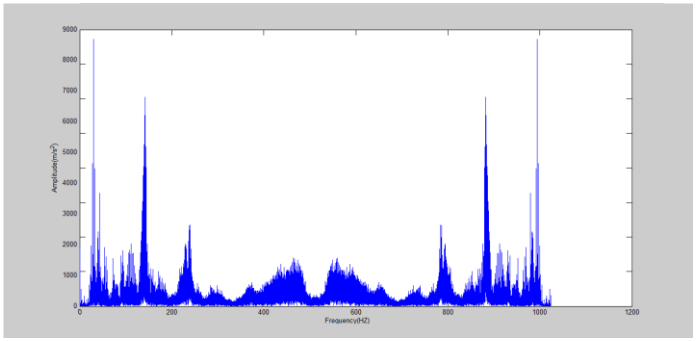


Figure 3.4 FFT plot(30% blockage, 10 Hz)

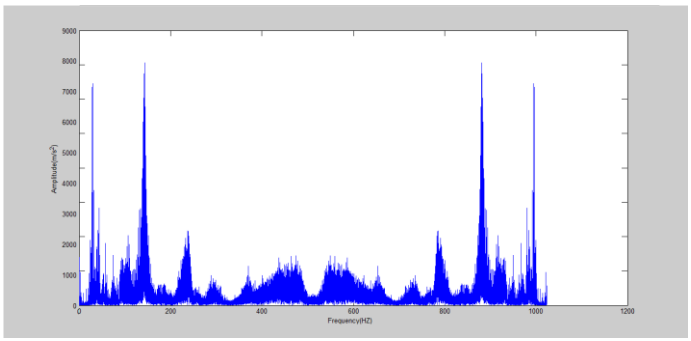

Figure 3.5 FFT plot (40% blockage, 10 Hz)

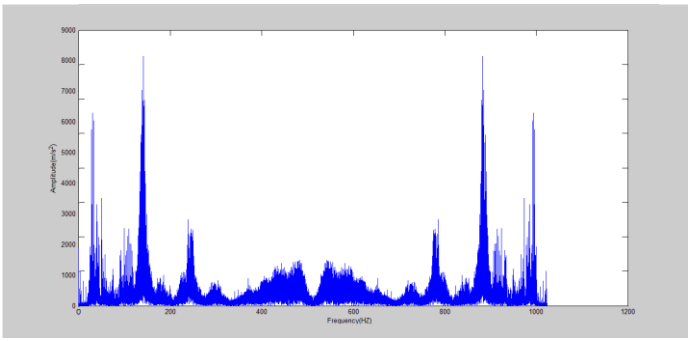

Figure 3.6 FFT plot(50% blockage, 10 Hz)

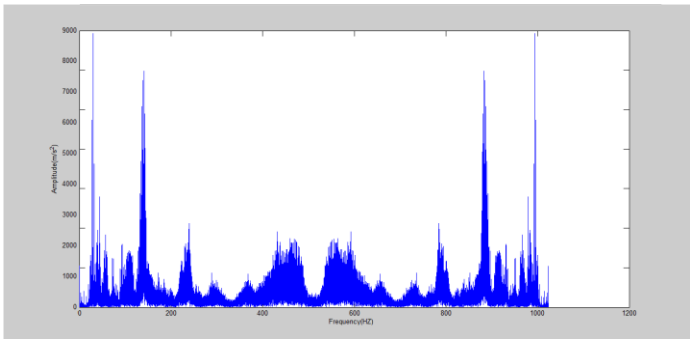

Figure 3.7 FFT plot (60% blockage, 10 Hz)

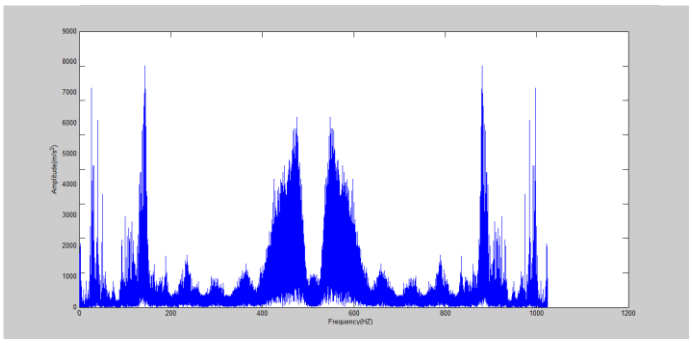

Figure 3.8 FFT plot(70% blockage, 10 Hz)

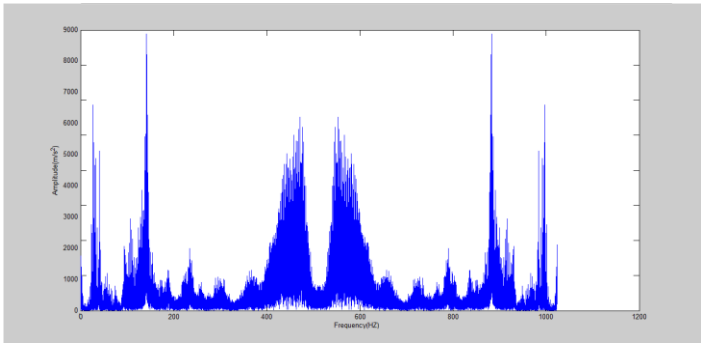

Figure 3.9 FFT plot (80% blockage, 10 Hz)

It can be seen that as we increase the blockage, the whole band of frequencies from 400-600 Hz increases in amplitude. The rest of the graph more or less remains unchanged. However, taking linear mean of the graph did not give good results in classification and powers of amplitude more than 2 also failed because it was classifying all the pairs with the same accuracy. This trend observed in the graph was the motivation to use

energy or squares of amplitudes (time being constant for all signals was not a factor) as a characterizing parameter in the ANN.

## 3.2 Accuracy of classification

The neural network toolbox was used and the extracted feature is input. The results obtained were from the toolbox interface were noted and tabulated.

The classifying accuracies in tabular form for 10%, 30%, 50%, and 70% with base 0% are given below

Table 3.1 Accuracy table for nnclass(b0, b10) at varying frequencies

| Frequency | Training Accuracy | Validation Accuracy | Testing Accuracy | Average Accuracy |
|---|---|---|---|---|
| 10 HZ | 66.14 | 66.66 | 66.33 | 66.3766 |
| 15 HZ | 69.34 | 64.1 | 71.2 | 68.21333333 |
| 20 HZ | 67.15 | 66.667 | 83.44 | 72.419 |
| 25 HZ | 71.98 | 70.22 | 65.87 | 69.35666667 |
| 30 HZ | 63 | 64.76 | 73.3334 | 67.03113333 |
| 35 HZ | 64.56 | 67.8 | 79 | 70.45333333 |
| 40 HZ | 69.98 | 68.65 | 72 | 70.21 |

In this first step of classification, it can be seen that not much accuracy is achieved. The average accuracy is around 63.953% and the range of accuracies is approximately from 66-70.45%. This is quite natural as a 10% blockage will not be as different from base 0% as a higher percentage blockage signal, like 30%. The increasing trend in accuracies is evident from the following tables,

Table 3.2 Accuracy table for nnclass(b0, b30) at varying frequencies

| Frequency | Training Accuracy | Validation Accuracy | Testing Accuracy | Average Accuracy |
|---|---|---|---|---|
| 10 HZ | 75.7322 | 61.98 | 70.11 | 69.27406667 |
| 15 HZ | 90 | 75.73 | 74.6 | 80.11 |
| 20 HZ | 67.15 | 66.667 | 83.44 | 72.419 |
| 25 HZ | 76.34 | 74.1 | 67.37 | 72.60333333 |
| 30 HZ | 76 | 74.12 | 72 | 74.04 |
| 35 HZ | 69.56 | 72.6 | 79 | 73.72 |
| 40 HZ | 75.38 | 88.65 | 71 | 78.34333333 |

The average accuracy is 74.353% and the range of accuracies is approximately from 69-80.11%.

Table 3.3 Accuracy table for nnclass(b0, b50) at varying frequencies

| Frequency | Training Accuracy | Validation Accuracy | Testing Accuracy | Average Accuracy |
|---|---|---|---|---|
| 10 HZ | 76 | 79.9 | 80 | 78.63333333 |
| 15 HZ | 85 | 80 | 86.87 | 83.95666667 |
| 20 HZ | 75.7 | 85.67 | 83.44 | 81.60333333 |
| 25 HZ | 88.98 | 80.22 | 85.87 | 85.02333333 |
| 30 HZ | 91 | 84.76 | 87.1 | 87.62 |
| 35 HZ | 84.14 | 87.8 | 81 | 84.31333333 |
| 40 HZ | 81.98 | 88.65 | 92 | 87.54333333 |

The average accuracy is 84.097% and the range of accuracies is approximately from 78.63-87.54%.

Table 3.4 Accuracy table for nnclass(b0, b70) at varying frequencies

| | Training Accuracy | Validation Accuracy | Testing Accuracy | Average Accuracy |
|---|---|---|---|---|
| 10 HZ | 82.8124 | 86.73 | 86.667 | 85.40313333 |
| 15 HZ | 94.219 | 93.334 | 100 | 95.851 |
| 20 HZ | 94.28579 | 95 | 100 | 96.42859667 |
| 25 HZ | 91.429 | 93.334 | 93.334 | 92.699 |
| 30 HZ | 88.58 | 92.84 | 86 | 89.14 |
| 35 HZ | 93.34 | 97.124 | 100 | 96.82133333 |
| 40 HZ | 98.18 | 98.65 | 80 | 92.27666667 |

The average accuracy is around 92.65% and the range of accuracies is approximately from 85.4-96.82%.

The implications and conclusions that can be drawn from the above mentioned tables are presented in the following section.

# Chapter 4

# CONCLUSIONS AND SCOPE FOR FUTURE WORK

## 4.1 Conclusions

The main objective of the report is to classify the degree of blockages. Experiments were performed on the MFS faulty compressor kit and using the energy feature of the Fourier transform plot, classification was done. The observations of classification accuracies were shown above. The following conclusions can be deduced from the observations,

1. It is found that the classification accuracies increase as x (blockage being classified) increases.
2. A slight deviation is found when the frequency is 10Hz for each combination of blockage because the compressor could not function properly at such small RPMs.
3. It can be seen that the average classification accuracy for each class differs by approximately 9.56 percentage points.
4. The following table displays the values of classification accuracies for each blockage and summarizes the results

| Degree of Blockage | Accuracy in classification with base 0% |
|---|---|
| 0-10% | 0-70.453% |
| 10-30% | 69.27-80.11% |
| 30-50% | 78.63-87.54% |
| 50-70% | 85.4-96.82% |

Table 4.1 Final Result Table of degree of blockage vs. accuracy

5. The blockage severity can be analyzed by taking the vibration reading of the faulty compressor and classifying it with base 0% blockage. The accuracy achieved in classifying the pair can be mapped in the following table and the corresponding degree of blockage can be found out.

## 4.2 Scope for future work

1. To increase the gap between classifying accuracies using other modes of decomposition like empirical mode decomposition, wavelet transform

2. To use multi class ANN to try and incorporate all classes in a single framework using increased number of input parameters including features like entropy, rms value.

3. To study the characteristics of valve leakage, also provided in the faulty compressor kit in a similar manner.

**Nomenclature**

| | |
|---|---|
| n | Output nodes for a given training pattern |
| Sj | Sum of all relevant products of weight and output from previous layer |
| aj | Activations of the nodes in the previous layer i, |
| $a_j$ | Activation of the node at hand, |
| f() | f is the activation function. |
| $E_p$ | Total error over the training pattern |
| $t_j$ | Represents the target value for node n in output layer j |
| E | Energy |
| T | Duration of signal |
| E | Total error |
| p | Represents all training patterns |
| P | Total number of training patterns |
| N | Total number of output nodes |
| MSE | Mean squared error |
| nnclass (,) | Neural Network classifier function |
| b0 | Energy matrix corresponding to 0% blockage |
| bx | Energy matrix corresponding to x% blockage where x=10,30,50,70 |

## *References*


[1]. L.H. Chiang, E.L.Rusell, R.D.Braatz, Fault Detection and Diagnosis in Industrial Systems, 1sted.Springer, London, UK, 2000.

[2]. B.C.Juricek, D.E.Seborg, W.E.Larimore, Fault detection using canonical variate analysis, Ind. Eng.Chem.Res.43(2)(2004)458–474.

[3]. A.Simoglou, E.B.Martin, A.J.Morris, Statistical performance monitoring of dynamic multivariate processes using states pace modelling, Comput. Chem. Eng.26(6)(2002)909–920.

[4]. M.Y.M.Yunus,J. Zhang, Multivariate process monitoring using classical multidimensional scaling and procrustes analysis, IFAC Proceedings Volumes (IFAC – Papers Online),vol.9,2010,pp.165.

[5]. K.Zhou, Q.Li,R. Guo,Improving monitoring accuracy of process based on SPC method, in:Proceedings of the 2012 24th Chinese Control and Decision Conference,CCDC2012,2012,p.1488.

[6]. A.Alkaya, İ. Eker,Variance sensitive eadaptive threshold-based PCA method for fault detection with experimental application, ISATrans.50(2)(2011) 287–302.

[7]. H.J.Borsje,Fault detection in boilers using canonical variate analysis,in:Proceedings of theA merican Control Conference, vol.2, 1999,p.1167.

[8]. P.Eserin, Application of canonical variate analysis to the dynamical modeling and control of drum level in an industrial boiler, in: Proceedings of the American ControlConference,vol.2,1999,p.1163.

[9]. H.W.Lee, M.W.Lee, J.M.Park, Multi-scale extension of PLS algorithm for advanced on-line process monitoring, Chemom. Intell.Lab.Syst.98(2)(2009) 201–212.

[10]. K.Peng, G.Li,K. Zhang, Strip thickness monitoring in hotstrip mill processes based on dynamic total projection to latent structures(T-PLS)algorithm, Kongzhi Li lun Yu Ying yong/ Control Theory Appl.29(11)(2012)1446–1451.

[11]. E.Vanhatalo, Multivariate process monitoring of an experimental blast furnace, Qual. Reliab.Eng.Int.26(5)(2010)495–508.

[12]. Y.Rotem, A.Wachs,D.R.Lewin, Ethylene compressor monitoring using model-based PCA,AIChEJ Cárceletal./MechanicalSystemsandSignalProcessing66-67(2016)699–714 713

[13]. T.Komulainen, M.Sourander, S.Jämsä-Jounela, An online application of dynamic PLS to ad aromatization process,Comput.Chem.Eng.28(12)(2004) 2611–2619.

[14]. W.Ku,R.H. Storer, C.Georgakis, Disturbance detection and isolation by dynamic principal component analysis, Chemom.Intell.Lab.Syst.30(1)(1995) 179–196.

[15]. E.L.Russell, L.H.Chiang, R.D.Braatz, Fault detection in industrial processes using canonical variate analysis and dynamic principal component analysis, Chemom. Intell.Lab.Syst.51(1)(2000)81–93.

[16]. P.P.Odiowei, Y.Cao, Non linear dynamic process monitoring using canonical variate analysis and kernel density estimations, Comput. Aided Chem. Eng. 27(C)(2009)1557–1562.

[17]. C.J.Stander, P.S.Heyns, W.Schoombie, Using vibration monitoring for local fault detection on gears operating under fluctuating load conditions, Mech. Syst.SignalProcess.16(6)(2002)1005–1024.

[18]. P.D.McFadden, Detecting fatigue cracks in gears by amplitude and phase demodulation of the meshing vibration,J.Vib.Acoust.StressReliab.Des.108 (2) (1986)165–170.

[19]. P.D.McFadden, Determining the location of a fatigue crack in a gear from the phase of the change in the meshing vibration, Mech. Syst. Signal Process. 2 (4)(1988)403–409.

[20]. G.Dalpiaz, A.Rivola, R.Rubini, Effectiveness and sensitivity of vibration processing techniques for local fault detection in gears, Mech. Syst. Signal Process.14(3)(2000)387–412.

[21]. N.Baydar, A.Ball, A comparative study of acoustic and vibration signals in detection of gear failures using Wigner–Ville distribution, Mech. Syst. Signal Process.15(6)(2001)1091–1107.

[22]. B.E.ParkerJr.,H.A.Ware,D.P.Wipf,W.R.Tompkins,B.R.Clark,E.C.Larson,H.V.Poor,Fault diagnostics using statistical change detection in the bispectral domain,Mech.Syst.SignalProcess.14(4)(2000)561–570.

[23]. Y.Zhan, V.Makis, A.K.S.Jardine, Adaptive state detection of gear boxes under varying load conditions based on parametric modelling, Mech. Syst. Signal Process.20(1)(2006)188–221.

[24]. S. Braun, The synchronous (timedomain) average revisited, Mech. Syst. Signal Process. 25(4)(2011)1087–1102.

[25]. W.Bartelmus, R.Zimroz, A new feature for monitoring the condition of gear boxes in non-stationary operating conditions, Mech. Syst. Signal Process. 23 (5)(2009)1528–1534.

[26]. R.Zimroz, W.Bartelmus, T.Barszcz, J.Urbanek, Diagnostics of bearings in presence of strong operating conditions non-stationarity—a procedure of load-dependent features processing with application to wind turbine bearings, Mech. Syst .Signal Process.46(1)(2014)16-27.

[27]. H.Cohen, G.F.C.Rogers, H.I.H.Saravanamuttoo, Gas Turbine Theory, fourth ed.AddisonWesleyLongmanLimited,Harlow,1996.

[28]. T.Gravdahl, O.Egeland, Compressor Surge and Rotating Stall: Modeling and Control, Springer Publishing Company, Incorporated, NewYork, 2011.

[29]. N.Lu, Z.H.Xiao, O.P.Malik, Feature extraction using adaptive multiwavelets and synthetic detection index for rotor fault diagnosis of rotating machinery, Mech.Syst.SignalProcess.52–53 (2015)393–415.

[30]. J.Wang, Q.B.He, F.R.Kong, Multi scale envelope manifold for enhanced fault diagnosis of rotating machines, Mech. Syst. Signal Process.52–53 (2015) 376–392.

[31]. N.Harish Chandra, A.S.Sekhar, Fault detection in rotor bearing systems using time frequency techniques, Mech. Syst. Signal Process.72–73(2016) 105–133.

[32]. N.R.Sakthivel, V.Sugumaran, S.Babudevasenapati, Vibration based fault diagnosis of monoblock centrifugal pump using decision tree, Expert Syst. Appl. 37(2010)4040–4049.

[33]. J.T.Cui, S.W.Wang, A model-based online fault detection and diagnosis strategy for centrifugal chiller systems, Int.J.Thermal Sci.44(2005)986–999.

[34]. I.Loboda, S.Yepifanov, A mixed data-driven and model based fault classification for gas turbine diagnosis, in:Proceedings of ASME Turbo Expo2010: Power for Land, Sea and Air,2010,pp.1–9.

[35]. M.J. Yang, Q.Shen, Reinforcing fuzzy rule-based diagnosis of turbo machines with case-based reasoning, Int.J.Knowl.-based Intel.Eng.Syst.12(2) (2008)173–181.

[36]. R.W.Eustace, A.Real-World, Application of fuzzy logic and influence coefficients for gas turbine performance diagnostics, J.Eng. Gas Turbines Power 130(2008).061601-1-061601-061609.

[37]. A.Hafaifa, K.Laroussi, F.Laaouad, Robust fuzzy fault detection and isolation approach applied to surge in centrifugal compressor modeling and control, Fuzzy Inform. Eng.2(1)(2010)49–73.

[38]. A.Azadeh, M.Saberi ,A.Kazem, et al., A flexible algorithm for fault diagnosis in a centrifugal pump with corrupted data and noise based on ANN and support vector machine with hyper-parameters optimization, Appl.Soft Comput.13(3)(2013)1478–1485.

[39]. W.Li, Z.C.Zhu, F.Jiang, et al, Fault diagnosis of rotating machinery with an ovel statistical feature extraction and evaluation method, Mech. Syst. Signal Process. 50–51 (2015)414–426.